WATER RESOURCES RESEARCH, VOL. 32, NO. 5, PAGES 1441–1448, MAY 1996

Influence of valley type on the scaling properties of river planforms

Anicet A. Beauvais
Institut Francais de Recherche Scientifique pour le Développement en Coopération, Bondy, France

David R. Montgomery
Department of Geological Sciences and Quaternary Research Center, University of Washington, Seattle

Abstract. Scaling properties of 44 individual river planforms from the Cascade and Olympic Mountains of Washington State were defined using the divider method. Analysis of the standardized residuals for least squares linear regression of Richardson plots reveals systematic deviations from simple self-similarity that correlate with the geomorphological

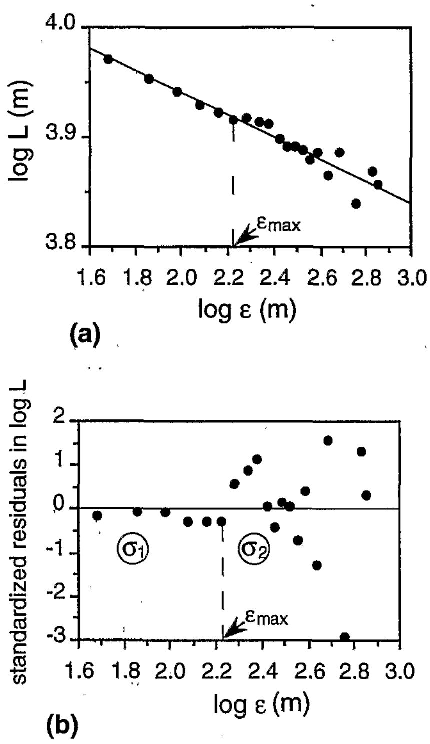

Figure 1. (a) Richardson plot characterized by a length scale ε_{max} above which the variance increases about the central tendency. (b) Definition of ε_{max} based on the variance (σ) of the standardized residuals of Richardson plot.

Nikora, 1991; *Gan et al.*, 1992; *Beauvais et al.*, 1994], as well as that of other geologic and geomorphologic features [e.g., *Goodchild*, 1980; *Aviles et al.*, 1987; *Brown*, 1987; *Culling and Datko*, 1987; *Andrle and Abrahams*, 1989; *Gilbert*, 1989; *Matsushita et al.*, 1991; *Power and Tullis*, 1991; *Klinkenberg and Goodchild*, 1992]. The divider method involves measuring the length L of a curve using a ruler or divider of variable length ε. If the curve exhibits fractal scaling, then the length of the curve is a power law function of ε, such that

$$L \cong b\varepsilon^{1-D} \tag{4}$$

where b is a proportionality constant. Typically, D is calculated from logarithmic plots of L versus ε, known as Richardson plots, using

$$\log L = \log b + (1 - D) \log \varepsilon \tag{5}$$

The slope of a Richardson plot defines D, which indicates how fast the river planform length increases as ε decreases [*Mandelbrot*, 1967]. The power law function defined by (5) holds at all scales for self-similar curves such as Koch or Peano curves [*Mandelbrot*, 1983] and describes statistically self-similar and self-affine curves only over a limited range of scales [*Mandelbrot*, 1985; *Matsushita and Ouchi*, 1989; *Nikora*, 1994].

Mandelbrot [1977] anticipated that many natural objects are described by several fractal dimensions identifiable over discrete scaling domains. *Dutton* [1981] later showed that irregular curves often are described by different fractal dimensions over discrete scaling ranges. Such ranges in scaling properties might reflect the scales over which specific phenomena or processes operate or dominate the form of a system [*Church and Mark*, 1980; *Lam and Quattrochi*, 1992]. *Nikora* [1991], for example, hypothesized that the river and valley width respectively define lower and upper limits for the application of fractal analysis to river planform geometry. Similarly, *Snow* [1989] argued that the scale of meander representation defines an upper limit for ε. Here we use the divider method to investigate the scaling properties of natural river planforms and explore their relation to the geomorphological context defined by valley type.

Methods

The divider method only applies over a limited range of scales, and misapplication can lead to inconsistent results [*Goodchild*, 1980]. Richardson plots obtained from the classical application of the divider method generally exhibit two scaling thresholds that bound the range of scales over which a single dimension is estimated using least squares linear regression. For river planforms, the smaller-scale cutoff (ε_{min}) is related to the width of the river simply because the river cannot meander at finer length scales. The upper limit to defining D from Richardson plots (ε_{max}) generally is taken to be the ε value above which the variance of residuals about the regression abruptly increases (Figure 1). These two limits define the range of scales over which fractal analysis can describe the geometry of an object measured to derive a Richardson plot.

A problem with the divider method is that the results are sensitive to the treatment of the remainder length at the end of the planform [*Aviles et al.*, 1987; *Klinkenberg and Goodchild*, 1992; *Andrle*, 1992]. Richardson plots also can exhibit deviations from simple power law scaling, as revealed by systematic curvature of the structure of the standardized residuals [*Andrle and Abrahams*, 1989; *Andrle*, 1992; *Klinkenberg and Goodchild*, 1992]. *Andrle* [1992] and *Klinkenberg* [1994] provide more in-depth discussions on the divider method.

Remainder Length

The number of "steps" (N) needed to traverse the length L of a curve is typically a noninteger, as a fractional ε length often remains at the end of the planform. This implies an increase in measurement error as ε increases. There are three ways to treat the remainder length using the divider method [*Aviles et al.*, 1987]: (1) add the remainder length to the estimate of L; (2) neglect the remainder length; and (3) round N up to the nearest whole number. *Aviles et al.* [1987] found that retaining the remainder length produced Richardson plots with slightly greater scatter and higher D values; and that rounding greatly increased the scatter in the plots. Here we further examine the influence of the first two approaches on estimates of D.

Curvature in Richardson Plots

The linearity of Richardson plots was examined according to the method of *Andrle* [1992] to test whether the fractal dimension is scale-independent. This method examines the curvature in the Richardson plots for deviation from strict self-similarity, using the standardized residuals from least squares linear regression of log L versus log ε [*Andrle and Abrahams*, 1989; *Andrle*, 1992]. If there was no structure to the regression residuals, then a single D was estimated using least squares linea regression of data between ε_{min} and ε_{max}. Richardson plo exhibiting systematic structure to regression residuals were e amined for distinct linear trends over length scales betwe ε_{min} and ε_{max} (Figures 2a and 2b). We then performed regressions over each range of ε values characterized by a linear structure of residuals in the original composite regression to estimate D over these more restricted scaling domains (Figures 2c and 2d).

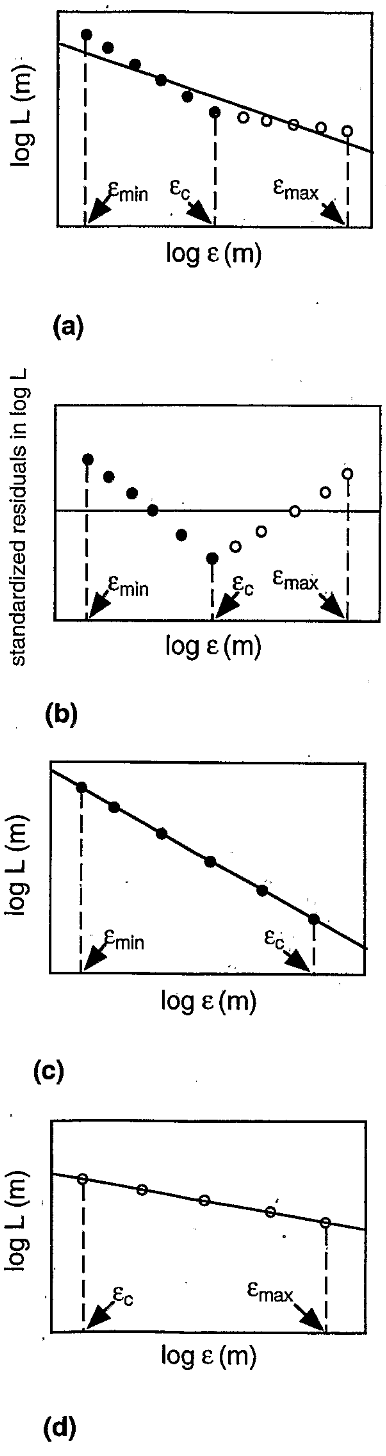

Figure 2. Illustration of the procedure for differentiating two scaling domains in Richardson plots. (a) An initial least squares linear regression of log L versus log ε is used to construct (b) a plot of the standardized residuals, which identifies scaling ranges well described by least squares linear regression over more restricted scaling ranges defined by (c) $\varepsilon_{min} < \varepsilon < \varepsilon_c$, and (d) $\varepsilon_c < \varepsilon < \varepsilon_{max}$.

Table 1. Fractal Scaling Properties and Sinuosity Characteristics of BV River Planforms Described by a Single Fractal Dimension D

River	D	σD	ε_{max}, m	A, m	λ, m
Cascades					
Chute Cr.	1.114	0.002	168	132	264
Clendenen Cr.	1.047	0.001	120	48	144
Gee Cr.	1.048	0.001	168	72	216
Hatchery Cr.	1.071	0.001	144	72	192
Little Deer Cr.	1.103	0.002	168	168	312
Little Deer Cr.*	1.076	0.001	144	72	192
Little Deer Cr.†	1.176	0.001	168	168	312
North Branch Cr.	1.079	0.001	144	60	216
O'Toole Cr.	1.044	0.001	168	48	192
Presentine Cr.	1.074	0.002	168	96	276
Quartz Cr.	1.095	0.001	168	108	264
DeForest Cr.	1.051	0.002	144	48	192
S. F. Nooksack R.	1.126	0.003	168	216	312
Olympics					
Alder Cr.	1.123	0.002	144	96	192
Braden Cr.	1.082	0.003	168	108	240
Cedar Cr.	1.101	0.001	168	156	264
Elk Cr.	1.061	0.001	216	72	240
S. F. Hoh R.*	1.069	0.001	144	144	240
Jackson Cr.	1.125	0.001	144	72	216
Lost Cr.	1.046	0.001	144	48	192
Maple Cr.	1.103	0.002	168	108	216
Mosquito Cr.†	1.172	0.004	192	168	420
Mount Tom Cr.	1.097	0.002	168	108	252
Owl Cr.	1.107	0.003	216	84	264
Steamboat Cr.	1.127	0.002	168	120	288
Winfield Cr.	1.125	0.003	168	132	264

BV; bedrock valley; σD, standard deviation of D; ε_{max}, upper limit of fractal scaling at which the divider method breaks down; A, largest meander amplitude; λ, largest meander wavelength; Cr., creek; R., river. Here $r^2 > 0.99$ for all the river analyses.

*Upstream reach.

†Downstream reach.

Procedure and Precision of the Divider Method

The precision of the divider method depends on both map scale and the smallest ε value used in the analysis. River planform lengths were measured manually using a compass from U.S. Geological Survey 1:24,000 scale topographic maps; measurement paths followed the centerline of the main channel. The smallest ε length equaled 2 mm (48 m), with subsequent measurements increasing at 1 mm (24 m) intervals of ε length (Figure 1a). The largest ε length used for each river equaled one tenth the total planform length. This procedure resulted in a large number of ε values, as recommended by *Andrle* [1992] for estimating D. Following *Andrle and Abrahams* [1989], replicate measurements on a number of rivers evaluated the precision of manual application of the divider method using a compass [*Richardson*, 1961; *Mandelbrot*, 1967, 1983; *Korvin*, 1992]. For all ε in the range of ε_{min} to ε_{max}, the number of compass walks in different measurement trials varied by at most 1% over the entire planform length.

Study Areas and River Characteristics

We analyzed 44 individual river planforms from Washington State. Twenty reaches are located in the Cascade Range, and 24 are from the Olympic Peninsula. Three types of reaches were defined based on valley-scale geomorphology (Tables 1–3). Twenty-six of the reaches flow through confined bedrock valleys (BV rivers), which have only a thin alluvial mantle over

Table 2. Fractal Scaling Properties and Sinuosity Characteristics of GV River Planforms Described by Two Fractal Dimensions With $D_s > D_l$

River	D_s	σD_s	D_l	σD_l	ε_c, m	ε_{max}, m	A, m	λ, m
Cascades								
Alder Cr.	1.134	0.002	1.070	0.001	82	360	120	360
Cumberland Cr.	1.121	0.002	1.051	0.001	96	288	108	300
Finney Cr.	1.229	0.002	1.106	0.001	157	408	216	432
Finney Cr.*	1.143	0.001	1.100	0.001	73	264	108	288
Grandy Cr.	1.149	0.002	1.060	0.002	63	264	84	312
Olympics								
Goodman Cr.	1.135	0.002	1.107	0.001	153	384	192	432
Goodman Cr.*	1.125	0.002	1.083	0.002	76	312	108	336
Minter Cr.	1.098	0.002	1.081	0.001	80	312	108	324
N. F. Mosquito Cr.	1.138	0.003	1.089	0.001	100	264	108	300
Mosquito Cr.	1.20	0.003	1.137	0.001	151	408	168	420

GV, glacial valley; D_s, small-scale fractal dimension; D_l, large-scale fractal dimension; ε_c, scaling threshold separating two fractal scalings characterized by two fractal dimensions. See Table 1 for additional information.
*Upstream reach.

Table 3. Fractal Scaling Properties and Sinuosity Characteristics of AV River Planforms Described by Two Fractal Dimensions with $D_s < D_l$

River	D_s	σD_s	D_l	σD_l	ε_c, m	ε_{max}, m	A, m	λ, m
Cascades								
Finney Cr.*	1.103	0.001	1.201	0.002	132	312	216	432
Finney Cr.†	1.122	0.002	1.205	0.001	155	264	156	360
Olympics								
Goodman Cr.*	1.168	0.003	1.245	0.001	362	408	192	432
S. F. Hoh R.	1.102	0.001	1.186	0.004	316	480	348	648
S. F. Hoh R.*	1.135	0.002	1.251	0.002	397	480	348	648
S. F. Hoh R.†	1.106	0.005	1.302	0.003	216	336	312	480
Bogachiel R.*	1.075	0.003	1.28	0.014	295	336	276	552
Snahapish R.	1.144	0.002	1.248	0.003	253	288	168	408

AV, alluvial valley. See Tables 1 and 2 for additional information.
*Downstream reach.
†Downstream shorter reach.

bedrock and thus lack floodplains (Table 1). Ten reaches are incised into glacial outwash filling narrow and relatively straight U-shaped valleys (GV rivers) (Table 2). Eight reaches flow through wide alluvial valleys (AV rivers) with large active floodplains (Table 3). Some of the AV rivers flow through areas glaciated during the Pleistocene, but these rivers are not closely confined by valley or terrace walls. Six of the largest rivers were partitioned into upstream and downstream reaches based on differences in channel gradient and width; in addition to composite analyses, each of these reaches was analyzed individually.

Sinuosity Characterization

Within each reach, we measured the wavelength (λ) and the amplitude (A) of the largest meander because they define natural length scales that can be identified objectively. Adopting the method of *Williams* [1986], we measured these parameters on individual meander apexes along each river planform using a rule and compass. Meander characteristics were compared to the scaling thresholds derived from Richardson plots to explore ties between scaling limits and geomorphological length scales.

Results

Richardson Plots

Richardson plots for each of our channel reaches exhibit increased variance of the standardized residuals with larger ε. An abrupt increase in the variance of the residuals defines the upper limit of application of the divider method (i.e., ε_{max}), and a narrow range of power law scaling characterizes each of the study reaches. As discussed above, each of the reaches exhibit structure to regression residuals that define domains more appropriately described by separate fractal dimensions in Richardson plots. The threshold separating these scaling domains, ε_c, is defined as the intercept of the two linear regressions determined from the residual structure of the composite regression (Figure 2). Examination of the standardized residuals of the Richardson plots reveals that neglecting the remainder length yields a lower variance and hence a better estimate of D at small length scales. Conversely, at larger length scales ($\varepsilon > \varepsilon_{max}$), neglecting the remainder length yields greater variance in L, and power law scaling breaks down. Within each scaling domain identified in our analysis, all the river planforms exhibit linear structures in the residual plots, as well as an equal number of positive and negative standardized residual values; all the regressions exhibit $r^2 > 0.99$ at the 95% level of confidence.

Richardson plots from our reaches exhibit either a single fractal dimension or two fractal dimensions defined over distinct scaling ranges. These scaling ranges are separated by a scaling threshold ε_c, with either $D_s > D_l$ or $D_s < D_l$, where D_s is the fractal dimension at scales below ε_c, and D_l is the fractal dimension at scales above ε_c (Tables 1–3). Nearly all the rivers studied are narrower than the minimum ruler length

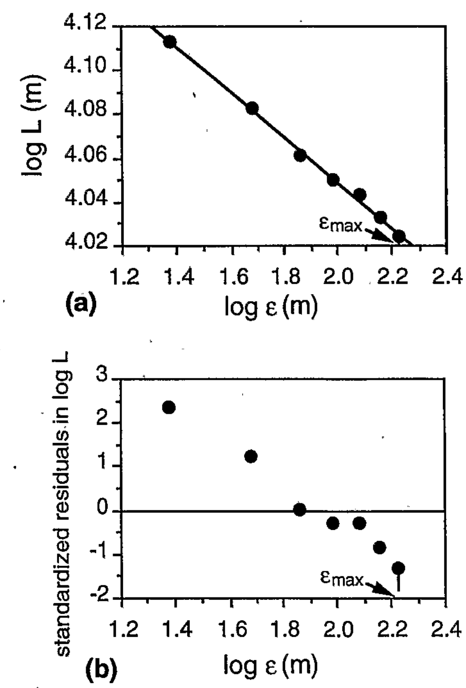

Figure 3. (a) Richardson plot of Little Deer Creek (BV river) described by a single fractal dimension, $D = 1.103$. (b) Standardized residuals of Richardson plot.

employed to measure the planform length L; only data from the widest AV river (South Fork Hoh River) exhibit a discernable lower cutoff ($\varepsilon_{min} \cong 120$ m).

The three valley types (BV, GV, and AV) are described by three different types of Richardson plots. The BV rivers that define the majority of our sample are described by a single fractal dimension that ranges from 1.04 to 1.18 (Table 1; Figures 1 and 3). The GV rivers exhibit $D_s > D_l$, with D_s ranging from 1.10 to 1.23, and D_l from 1.05 to 1.14 (Table 2; Figure 4). In contrast, the AV rivers are described by $D_s < D_l$, with D_s ranging from 1.08 to 1.17, and D_l from 1.19 to 1.30 (Table 3 and Figure 5). At short ε length scales, the BV and AV rivers have similar fractal dimensions, while the GV rivers are described by higher D values. At large ε length scales, the fractal dimension of AV rivers exceeds that of the GV rivers. GV and AV rivers exhibit ε_{max} values roughly double those of BV rivers. AV rivers further exhibit a transition scaling threshold (ε_c), as well as maximum meander amplitudes and wavelengths roughly twice those of GV rivers.

Among the river planforms partitioned into upstream and downstream reaches, the upstream sections of these reaches are described by a lower D than the downstream sections (Figures 6 and 7). Upstream reaches correspond either to BV rivers with low D or to GV rivers described by $D_s > D_l$, while downstream reaches correspond either to BV rivers with larger D or to AV rivers described by $D_s < D_l$.

Scaling Thresholds and Sinuosity

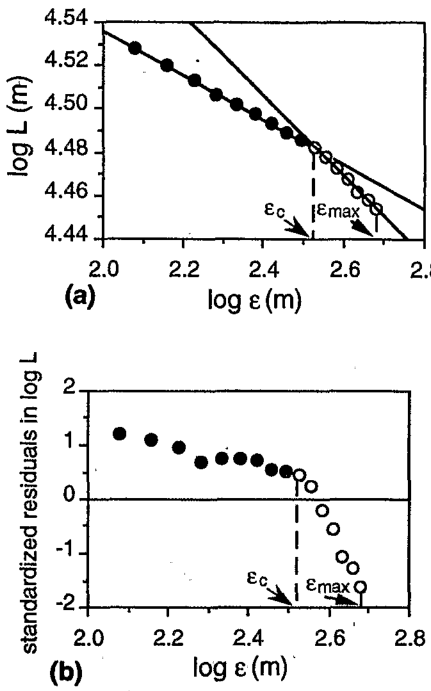

Figure 5. (a) Richardson plot of South Fork Hoh River (AV river) described by two fractal dimensions $D_s = 1.102$ and $D_l = 1.186$. (b) Standardized residuals for the composite regression displaying two distinct straight line structures defin-

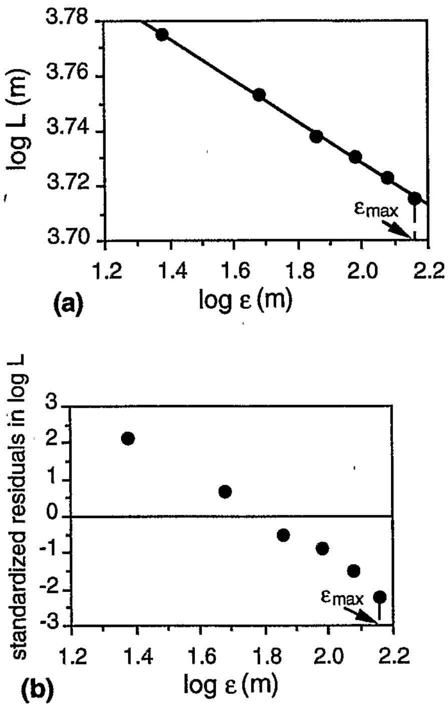

Figure 6. (a) Richardson plot of the upstream section of Little Deer Creek (BV river) described by a single fractal dimension $D = 1.076$. (b) Standardized residuals of Richardson plot.

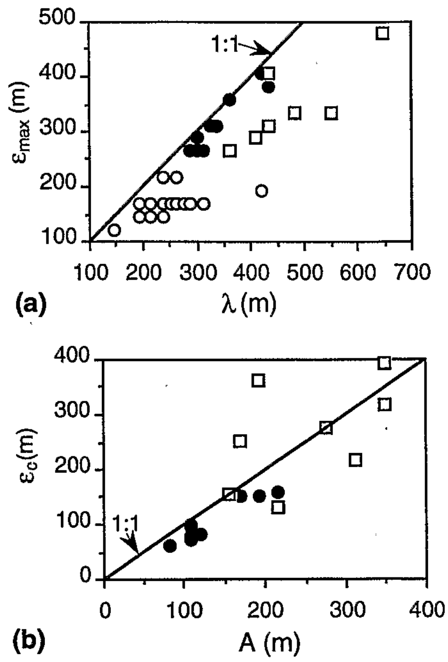

Figure 8. Correlation diagrams of (a) ε_{max} versus maximum meander wavelength (λ) and (b) ε_c versus maximum meander amplitude (A) (open circles, BV river data; solid circles, GV river data; squares, AV river data). Lines represent 1:1 relations; regression equations are collated in Table 4.

valley morphology. The channel width and the largest meander wavelength bound these scaling domains over which fractal geometry describes river planforms. This narrow scale range demonstrates that though river planforms may be self-affine, they are strictly self-similar only over a restricted range of scales.

The interplay of water flow, sediment transport, bed topography, and the nature of channel bank material controls meander development. Although some aspects of river planform geometry may reflect random processes [*Langbein and Leopold*, 1966; *Thakur and Scheidegger*, 1970; *Ghosh and Scheidegger*, 1971; *Shreve*, 1969, 1974; *Ferguson*, 1976; *Wallis*, 1978; *Turcotte*, 1992], the form and scale of meander patterns depend on interactions among channel gradient, valley floor material and the ratio of the river width to the valley width [*Wolman and Leopold*, 1957; *Bagnold*, 1960; *Leopold and Wolman*, 1960; *Schumm*, 1963; *Ferguson*, 1975; *Hey*, 1976; *Davies and Tinker*, 1984; *Williams*, 1986]. The form and size of meanders also depend on the river width-to-depth ratio, discharge, and the hydraulic properties of flow through bends [*Dury*, 1955, 1969; *Einstein and Shen*, 1964; *Engelund and Skovgaard*, 1973; *Ferguson*, 1975; *Parker*, 1976; *Dietrich et al.*, 1979; *Howard and*

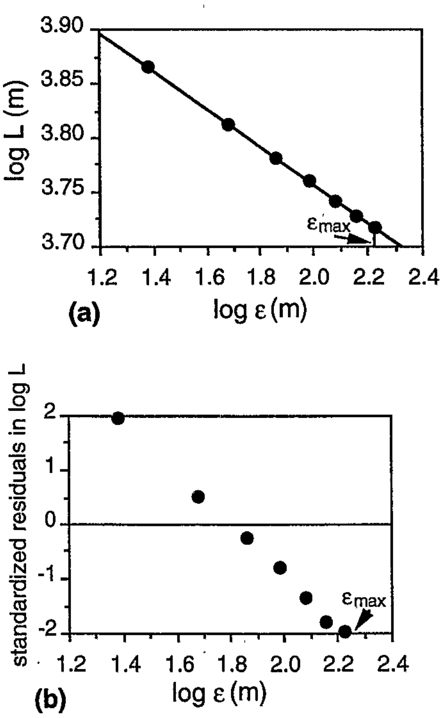

Figure 7. (a) Richardson plot of the downstream section of Little Deer Creek (BV river) described by a single fractal dimension $D = 1.176$. (b) Standardized residuals of Richardson plot.

Table 4. Relations Between Fractal Scaling and Meander Features

	ε_{max} Versus λ	ε_c Versus A
All data	$\varepsilon_{max} = 72.8 + 1.02\lambda$; $r = 0.85$	$\varepsilon_c = -9.4 + 0.99A$; $r = 0.81$
BV rivers	$\varepsilon_{max} = 109 + 0.22\lambda$; $r = 0.58$	...
GV rivers	$\varepsilon_{max} = -20.6 + 0.99\lambda$; $r = 0.96$	$\varepsilon_c = -0.76 + 0.79A$; $r = 0.94$
AV rivers	$\varepsilon_{max} = 39.4 + 0.65\lambda$; $r = 0.86$	$\varepsilon_c = 11.9 + 0.57A$; $r = 0.49$

Least squares linear regression equations of Figure 8 plots. BV, bedrock valley; GV, glacial valley; AV, alluvial valley.

Hemberger, 1991]. Our results indicate that the morphological signature of these processes defines the range of scales over which fractal geometry describes river planforms.

The relation between a channel and its valley helps explain the different scaling patterns of BV, AV, and GV rivers. BV rivers occupy narrow, confined valleys in which bedrock structure, strength, and fracture patterns may influence channel orientation. Resistant bedrock valley walls impede meandering, leading to quasi-linear planforms described by a single low D. The single D implies a lack of a preferential scale to the planform of bedrock rivers. GV rivers confined within incised glacial terraces meander freely at short length scales within the valley, but the inherited glacial form constrains channel form at larger scales. This restriction at large scales results in higher D at short wavelengths and lower D at longer wavelengths. In contrast, AV rivers occupying wide floodplains typically have low gradients and unconsolidated bank material that encourage meander development, and meander wavelength is proportional to discharge [*Dury*, 1955, 1969; *Carlston*, 1965; *Ikeda et al.*, 1981; *Richards*, 1982]. Although AV rivers are free to meander at all length scales, the lower D observed at shorter length scales documents simpler fine-scale channel form. We infer that the transitional scale (i.e., ε_c) represents that scale above which random influences dominate channel pattern and below which the interplay of flow hydraulics and sediment

Aviles, C. A., C. H. Scholz, and J. Boatwright, Fractal analysis applied to characteristic segments of the San Andreas fault, *J. Geophys. Res.*, *92*(B1), 331–344, 1987.

Bagnold, R. A., Some aspects of the shape of river meanders, *U.S. Geol. Survey Prof. Pap. 282E*, 135–144, 1960.

Beauvais, A., J. Dubois, and A. Badri, Application d'une analyse fractale à l'étude morphométrique du tracé des cours d'eau: méthode de Richardson, *C. R. Acad. Sci. Paris, Ser. II*, *318*, 219–225, 1994.

Brown, S. R., A note on the description of surface roughness using fractal dimension, *Geophys. Res. Lett.*, *14*, 1095–1098, 1987.

Carlston, C. W., The relation of free meander geometry to stream discharge and its geomorphic implications, *Am. J. Sci.*, *263*, 864–885, 1965.

Church, M., and D. M. Mark, On size and scale in geomorphology, *Prog. Phys. Geogr.*, *4*, 342–390, 1980.

Culling, W. E. H., and M. Datko, The fractal geometry of the soil-covered landscape, *Earth Surf. Processes Landforms*, *12*, 369–385, 1987.

Davies, T. R. H., and C. Tinker, Fundamental characteristics of stream meanders, *Geol. Soc. Am. Bull.*, *95*, 505–512, 1984.

Dietrich, W. E., and J. D. Smith, Influence of the point bar on flow through curved channels, *Water Resour. Res.*, *19*, 1173–1192, 1983.

Dietrich, W. E., J. D. Smith, and T. Dunne, Flow and sediment transport in a sand bedded meander, *J. Geol.*, *87*, 305–315, 1979.

Dury, G. H., Bedwidth and wavelength in meandering valleys, *Nature*, *176*, 31, 1955.

Dury, G. H., Relation of morphometry to runoff frequency, in *Water, Earth and Man*, edited by R. J. Chorley, pp. 419–430, Methuen, London, 1969.

Dutton, G. H., Fractal enhancement of cartographic line detail, *Am-*

La Barbera, P., and R. Rosso, On the fractal dimension of river networks, *Water Resour. Res.*, *25*, 735–741, 1989.

Lam, N. S.-N., and D. A. Quattrochi, On the issues of scale resolution and fractal analysis in the mapping sciences, *Prof. Geogr.*, *44*, 88–98, 1992.

Langbein, W. B., and L. B. Leopold, River meanders: Theory of minimum variance, *U.S. Geol. Surv. Prof. Pap.*, *422H*, 1966.

Leopold, L. B., and M. G. Wolman, River meanders, *Geol. Soc. Am. Bull.*, *71*, 769–784, 1960.

Leopold, L. B., M. G. Wolman, and J. P. Miller, Fluvial processes in geomorphology, 522 pp., W. H. Freeman, New York, 1964.

Lovejoy, S., D. Schertzer, and A. A. Tsonis, Functional box counting and multiple elliptical dimensions in rain, *Science*, *235*, 1036–1038, 1987.

Mandelbrot, B. B., How long is the coast of Britain?: Statistical self-similarity and fractional dimension, *Science*, *155*, 636–638, 1967.

Mandelbrot, B. B., *Fractals: Form, Chance and Dimension*, 365 pp., W. H. Freeman, New York, 1977.

Mandelbrot, B. B., *The Fractal Geometry of Nature*, 468 pp., W. H. Freeman, New York, 1983.

Mandelbrot, B. B., Self-affine fractals and fractal dimension, *Phys. Scr.*, *32*, 257–260, 1985.

Mark, D. M., and P. B. Aronson, Scale-dependent fractal dimension of topographic surfaces: An empirical investigation, with applications in geomorphology and computer mapping, *Math. Geol.*, *16*, 671–683, 1984.

Matsushita, M., and S. Ouchi, On the self-affinity of various curves, *Physica D*, *38*, 246–251, 1989.

Matsushita, M., S. Ouchi, and K. Honda, On the fractal structure and statistics of contour lines on a self-affine surface, *J. Phys. Soc. Jpn.*, *60*, 2109–2112, 1991.

Montgomery, D. R., and W. E. Dietrich, Channel initiation and the problem of landscape scale, *Science*, *255*, 826–830, 1992.

Nikora, V. I., Fractal structures of river planforms, *Water Resour. Res.*, *27*, 1327–1333, 1991.

Nikora, V. I., On self-similarity and self-affinity of drainage basins, *Water Resour. Res.*, *30*, 133–137, 1994.

Nikora, V. I., V. B. Sapozhnikov, and D. A. Noever, Fractal geometry of individual river channels and its computer simulation, *Water Resour. Res.*, *29*, 3561–3568, 1993.

Parker, G., On the cause and characteristic scales of meandering and braiding, *J. Fluid Mech.*, *76*, 457–480, 1976.

Phillips, J. D., Interpreting the fractal dimension of river networks, *In Fractals in Geography*, vol. 7, edited by N. S. Lam and L. De Cola, pp. 142–157, Prentice-Hall, Englewood Cliffs, N. J., 1993.

Power, W., and T. Tullis, Euclidean and fractal models for the description of rock surface roughness, *J. Geophys. Res.*, *96*, 415–424, 1991.

Richards, K., *Rivers: Form and Process in Alluvial Channels*, 358 pp., Methuen, New York, 1982.

Richardson, L. F., The problem of contiguity: an appendix to "Statistics of deadly quarrels," *Gen. Syst. Yearb.*, *6*, 139–187, 1961.

Robert, A., and A. Roy, On the fractal interpretation of the mainstream length drainage area relationship, *Water Resour. Res.*, *26*, 839–842, 1990.

Rosso, R., B. Bacchi, and P. La Barbera, Fractal relation of mainstream length to catchment area in river networks, *Water Resour. Res.*, *27*, 381–387, 1991.

Schumm, S. A., Evolution of a drainage systems and slopes in badlands at Perth Amboy, New Jersey, *Geol. Soc. Am. Bull.*, *67*, 597–646, 1956.

Schumm, S. A., Sinuosity of alluvial rivers on the great plains, *Geol. Soc. Am. Bull.*, *74*, 1089–1100, 1963.

Shreve, R. L., Stream lengths and basin areas in topologically random channel networks, *J. Geol.*, *77*, 397–414, 1969.

Shreve, R. L., Variation in mainstream length with basin area in river networks, *Water Resour. Res.*, *10*, 1167–1177, 1974.

Snow, R. S., Fractal sinuosity of stream channels, *Pure Appl. Geophys.*, *131*, 99–109, 1989.

Tarboton, D. G., R. L. Bras, and I. Rodriguez-Iturbe, The fractal nature of river networks, *Water Resour. Res.*, *24*, 1317–1322, 1988.

Thakur, T. R., and A. E. Scheidegger, Chain model of river meanders, *J. Hydrol.*, *12*, 25–47, 1970.

Turcotte, D. L., *Fractals and Chaos in Geology and Geophysics*, 221 pp., Cambridge Univ. Press, New York, 1992.

Wallis, I. G., The random component in stream meandering, *Water Resour. Bull.*, *14*, 576–586, 1978.

Williams, G. P., Rivers meanders and channel size, *J. Hydrol.*, *88*, 147–164, 1986.

Wolman, M. G., and L. B. Leopold, River floodplains: Some observations on their formation, *U.S. Geol. Surv. Prof. Pap. 182C*, 87–109, 1957.

Woronow, A., Morphometric consistency with the Hausdorff-Besicovich dimension, *Math. Geol.*, *13*(3), 201–216, 1981.

A. A. Beauvais, ORSTOM, Centre d'Ile de France, 32 av. Henri Varagnat, 93143 Bondy Cedex, France. (e-mail: beauvais@bondy.orstom.fr)

D. R. Montgomery, Department of Geological Sciences and Quaternary Research Center, University of Washington, Seattle, WA 98195-1310.

(Received May 19, 1995; revised January 10, 1996;
accepted January 18, 1996.)